*Int. J. Morphol.,*
*42(6)*:1517-1523, 2024.

# Neuronal Architecture of Flexor and Extensor Muscle Co-activation During Elbow Flexion Revealed by PRV Tracing

## Arquitectura Neuronal de la Coactivación de los Músculos Flexores y Extensores Durante la Flexión del Codo Revelada por el Trazado PRV

**Yunshan Li[1]; Yi Li[1];Rongbo Shen[2]; Lu Yang[1]; Siyuan Huang[2]; Nana Xiao[2]; Feng Yuan[2] & Shengbo Yang[3]**

**LI, Y.; LI, Y.; SHEN, R.; YANG, L.; HUANG, S.; XIAO, N.; YUAN, F. & YANG, S.** Neuronal architecture of flexor and extensor muscle co-activation during elbow flexion revealed by PRV tracing. *Int. J. Morphol., 42(6)*:1517-1523, 2024.

**SUMMARY:** The regulatory mechanisms underlying the co-contraction of the biceps and triceps brachii muscles during elbow flexion remain unclear. This study aimed to elucidate the structural connections between nerve cells responsible for this co-activation. We employed the modified Sihler's staining technique to visualize the nerve-dense regions within the biceps and triceps brachii muscles. Additionally, a retrograde tracer (pseudorabies virus) expressing enhanced green and red fluorescent proteins was injected into these regions to map the structural relationships of nerve cells in the spinal cord, red nucleus of the midbrain, and the M1 region of the cerebral cortex. The nerve-dense regions in the biceps and triceps brachii muscles were located at 74.75 % and 61.90 % of muscle length, respectively. Three days post-injection, we observed single-labeled motor neurons innervating the biceps (green) and triceps (red), as well as double-labeled interneurons in the anterior horn of the spinal cord. Six days after injection, single- and double-labeled neurons were identified in the red nucleus and the M1 cortex. The presence of double-labeled neurons in both the spinal cord and brain regions provides evidence for the neural basis of co-activation in flexor and extensor muscles during elbow flexion. This study advances our understanding of the neural mechanisms controlling muscle co-contraction.

**KEY WORDS: Biceps brachii muscle; Triceps brachii muscle; Co-activation; interneuron; Neuronal cell architecture.**

## INTRODUCTION

Traditionally, it is understood that during elbow flexion, the biceps muscle contracts while the triceps muscle relaxes, a phenomenon known as reciprocal inhibition (Kagamihara & Tanaka, 1985). This mechanism involves the excitation of motor neurons innervating the agonist muscle and the inhibition of these innervating the antagonist muscle (triceps), facilitated by inhibitory interneurons in the spinal cord (Hirabayashi *et al*., 2020). Recent studies, however, have revealed that the triceps brachii is also coactivated during the late stages of elbow flexion to stabilize the joint (Lewis *et al*., 2010; Pincivero *et al*., 2019), indicating a more complex neuromodulatory process directed by the cerebral cortex to maintain joint stability (Chiou *et al*., 2013; Griffin *et al*., 2015).

In the movement of skeletal muscles innervated by the corticospinal tract, most muscle contractions are regulated by groups of interneurons before the descending fibers of the primary motor cortex (M1 area) neurons reach the anterior horn of the spinal cord (Canedo, 1997; Lanuza *et al*., 2004); however, there remains a lack of consensus on how the motor cortex regulates the coordinated contraction of antagonistic muscle groups. Specifically, the precise mechanisms by which the corticospinal tract and associated interneurons contribute to this co-activation are not well understood. Our research team hypothesized that the motor cortex may coordinate this co-activation through neurons in the M1 region that simultaneously excite both flexor and extensor muscles or through shared spinal cord interneurons.

[1] Department of Clinical Medicine, Grade 2019, Zunyi Medical University, Zunyi, People's Republic of China.
[2] Department of Clinical Medicine, Grade 2021, Zunyi Medical University, Zunyi, People's Republic of China.
[3] Department of Human Anatomy, Zunyi Medical University, Zunyi 563099, People's Republic of China.

**FUNDING.** This work were supported by the National Natural Science Foundation of China, Grant/Award Number: 32260217; and Science and Technology Projects of Guizhou Province, Grant/Award Number: ZK[2023]056; and Zunyi Medical University Student Innovation Project, Grant/Award Number: S202210661112.

Received: 2024-08-08 Accepted: 2024-08-25

However, anatomical evidence supporting this hypothesis is currently lacking.

To address this gap, this study utilized Sihler's staining to visualize intramuscular nerve-dense regions (INDRs) in the biceps and triceps muscles (Yu *et al*., 2023). We then employed a pseudorabies virus (PRV) expressing enhanced green and red fluorescent proteins to trace the retrograde pathways of nerve cells innervating these muscles. This approach aimed to clarify the structural relationships between these nerve cells and provide morphological evidence to elucidate the regulatory mechanisms underlying muscle co-activation during elbow flexion.

## MATERIAL AND METHOD

**Experimental animals and ethics:** We used 42 (half males and half females) adult Sprague–Dawley (SD) rats (SPF grade), weighing 180 ± 20 g, obtained from the Laboratory Animal Center of Zunyi Medical University. Of these, 6 rats were used for intramuscular nerve staining, and 36 rats were used for retrograde tracing of neuronal cell architecture. All procedures involving animals were approved by the Experimental Animal Ethics Committee of Zunyi Medical University (Production No. SCXK-2021-0002; Use No. SYXK-2021-0004; Laboratory Animal Quality Certificate No. 5621020622030; Ethical Approval No. ZMU21-2202-116).

**Gross anatomy:** Following intraperitoneal injection of 4 % pentobarbital sodium for anesthesia, the posterior neck skin of the rats was incised and dissected layer-by-layer to expose the C5-T1 segments of the spinal cord. The brachial plexus was isolated, and the musculocutaneous and radial nerves were exposed at the entry points into the biceps and triceps brachii muscles. Both muscles were then removed for subsequent nerve staining.

**Modified Sihler's intramuscular nerve staining.** In order to improve the accuracy of tracer injection, Sihler's staining was applied to display the intramuscular nerves dense region. The biceps and triceps (excluding the medial head of the triceps, because it is too small to be injected) from six rats were fixed in 10 % formaldehyde for 1 month. The modified Sihler's staining process was as follows: (1) Depigmentation: maceration in 3 % potassium hydroxide with 0.2 % hydrogen peroxide for 2-3 weeks. (2) Decalcification: In Sihler's solution I (1part glacial acetic acid, 2 parts glycerol, 12 parts 1 % chloral hydrate) for 4 weeks. (3) Staining: In Sihler's solution II (1 part Ehrlich stain, 2 parts glycerol, 12 parts 1 % chloral hydrate) for 4 weeks. (4) Destaining: In Sihler's solution I for 6-20 h. (5) Neutralization: In 0.05 % lithium carbonate for 2 h. (6) Transparentization: In a gradient of glycerol (40 %, 60 %, 80 %, and 100 %) for 1 week at each concentration. Nerve branch distribution patterns were observed on an X-ray film viewer to locate the center of the intramuscular nerve-dense regions (INDRs).

**PRV retrograde tracing:** Following anesthesia with intraperitoneal 4 % pentobarbital sodium (1mL/100 kg), the skin over the upper arm was incised to expose the biceps brachii and triceps muscles. According to the concentration and injection dose standards of PRV provided in the instruction manual, using a micro syringe, 3 μL of a PRV solution (2 x$10^9$ PFU/mL, Wuhan Shumi Brain Science Technology Co., Ltd., China) was injected slowly (over 10-30 min) into the center of the INDRs identified by Sihler's staining. The needle was left in place for 15 min post-injection.

PRV injections were divided into the following groups: (1) injection of a single muscle for tracer labeling, PRV-CAG EGFP (green) was injected into the biceps of 12 rats, and PRV-CAG mRFP (red) was injected into the triceps of 12 rats. Neuronal cell architecture of the spinal cord and brain was observed 3 and 6 days after injection, respectively; (2) Simultaneous injection of both muscles for tracer labeling: PRV-CAG-EGFP (green) and PRV-CAG-mRFP (red) were injected into the biceps and triceps of 12 rats, respectively. Neuronal cell architecture in the spinal cord and brain was observed 3 and 6 days after injection, respectively.

Rats were house individually, with free access to food and water. Buprenorphine (0.02 mg/kg) (Tianjin Pharmaceutical Research Institute Co., Ltd., China) was administered every 8-12 h for analgesia.

**Tissue Processing.** After 3 or 6 days, rats were euthanized under sodium pentobarbital anesthesia. The chest cavity was quickly opened, and the heart was exposed. An infusion needle was inserted into the ascending aorta via the left ventricle, and the right auricle was cut open. The system was flushed with 150 mL of normal saline followed by 500 mL of 0.1 mol/L phosphate buffer solution (pH 7.4) containing 4 % paraformaldehyde for fixation. The infusion was completed within 4 h.

The C5-T1 spinal cord segments, brainstem, and brain were removed, stored in 0.1 mol/L phosphate buffer solution (pH 7.4) with sucrose (15 %, 20 % and 30 %) for gradient dehydration, and placed in a 4 °C refrigerator until the tissue completely sank. Frozen sections (30 μm thick) were prepared, temporarily stored in 0.1 mol/L phosphate buffer (pH 7.4), dried in the dark, and sealed with 50 % glycerol. Sections were observed under a fluorescence microscope and photographed to analyze neuronal architecture.

**Statistical analysis.** The experimental data were processed using IBM SPSS statistical software (version 29.0; IBM Corporation, Armonk, N.Y., USA). The data of the intramuscular nerves dense region and the center point were expressed as percentages (mean ± SD)% to eliminate individual differences. The measurement data were confirmed to be normally distributed. Paired *t*-test was used to compare the data of the left and right sides; an independent sample t-test was used to compare males with females, with $P > 0.05$ indicating no significant difference.

## RESULTS

**Gross anatomical observation.** The brachial plexus nerves in the rats originated primarily from the C5-T1 nerve roots. The musculocutaneous nerve traveled from the dorsal surface of the short head of the biceps brachii, merging with the long and short heads of the muscle belly. It then bifurcated into two branches before entering the muscle. The radial nerve coursed obliquely posteriorly and inferiorly between the upper end of the medial head of the triceps brachii and the short head of the biceps brachii. It then divided into three branches and entered the triceps brachii from the posterior surfaces of its three heads (Fig. 1).

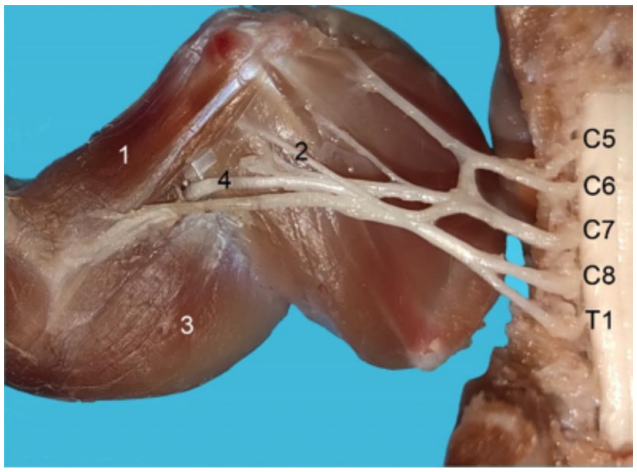


Fig. 1. Gross anatomy of the innervation of the biceps and triceps brachii muscles: 1: biceps brachii muscle; 2: musculocutaneous nerve; 3: triceps brachii muscle; 4: radial nerve.

**Sihler's staining and localization of intramuscular nerve-dense regions.** In the biceps brachii, the musculocutaneous nerve entered both the long and short heads. The short head branch exhibited fewer branches, while the long head branch showed a more extensive network of intramuscular dendritic branches, forming a triangular INDR located approximately (54.55±1.24) % to (85.25±1.79) % of the muscle length, with the center positioned (74.75±1.05) % of the muscle length (Figs. 2A and 2B). In the triceps brachii, the radial nerve branches were most numerous in the long head, which a dense distribution between (42.67±1.49) % and (81.12±1.60) % of the muscle length, centered at (61.90±1.35) % of the muscle length (Figs. 2C and 2D). There were no differences in nerve distribution patterns between sexes and between left and right sides.

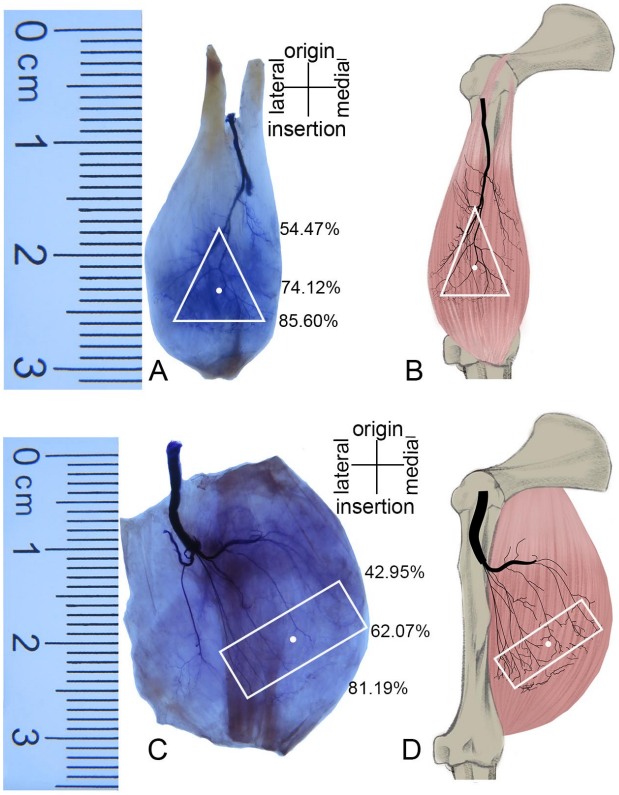


Fig. 2. Sihler's staining of biceps and triceps brachii muscles: A: superficial view of Sihler staining of the biceps, showing INDR (white triangular frame) and center point (white dot). B: Pattern diagram of A. C: superficial view of Sihler's staining of the triceps, showing INDR (white rectangular frame) and center point (white dot). D: Pattern diagram of C.

## PRV retrograde tracing

**Single muscle injection.** Three days after PRV-CAG-EGFP was injected into the biceps brachii and PRV-CAG-mRFP into the triceps brachii, PRV-infected star-shaped or triangular neurons were observed in the C5-T1 segments of the spinal cord. Six days post-injection, pyramidal cells were invisible in the M1 region of the cerebral cortex, predominantly on the ipsilateral side for the spinal cord and the contralateral side for the cerebral cortex. Neurons innervating the biceps brachii were green (Figs. 3A and 3B), while those innervating the triceps brachii were red (Figs. 3C and 3D). Fluorescent cells in the spinal cord were mainly concentrated in lamina VIII and IX of the C5-C8 (biceps brachii) and C5-T1 (triceps brachii) segments. Red-labeled cells in the spinal and cerebral cortices were slightly fewer than green-labeled cells.

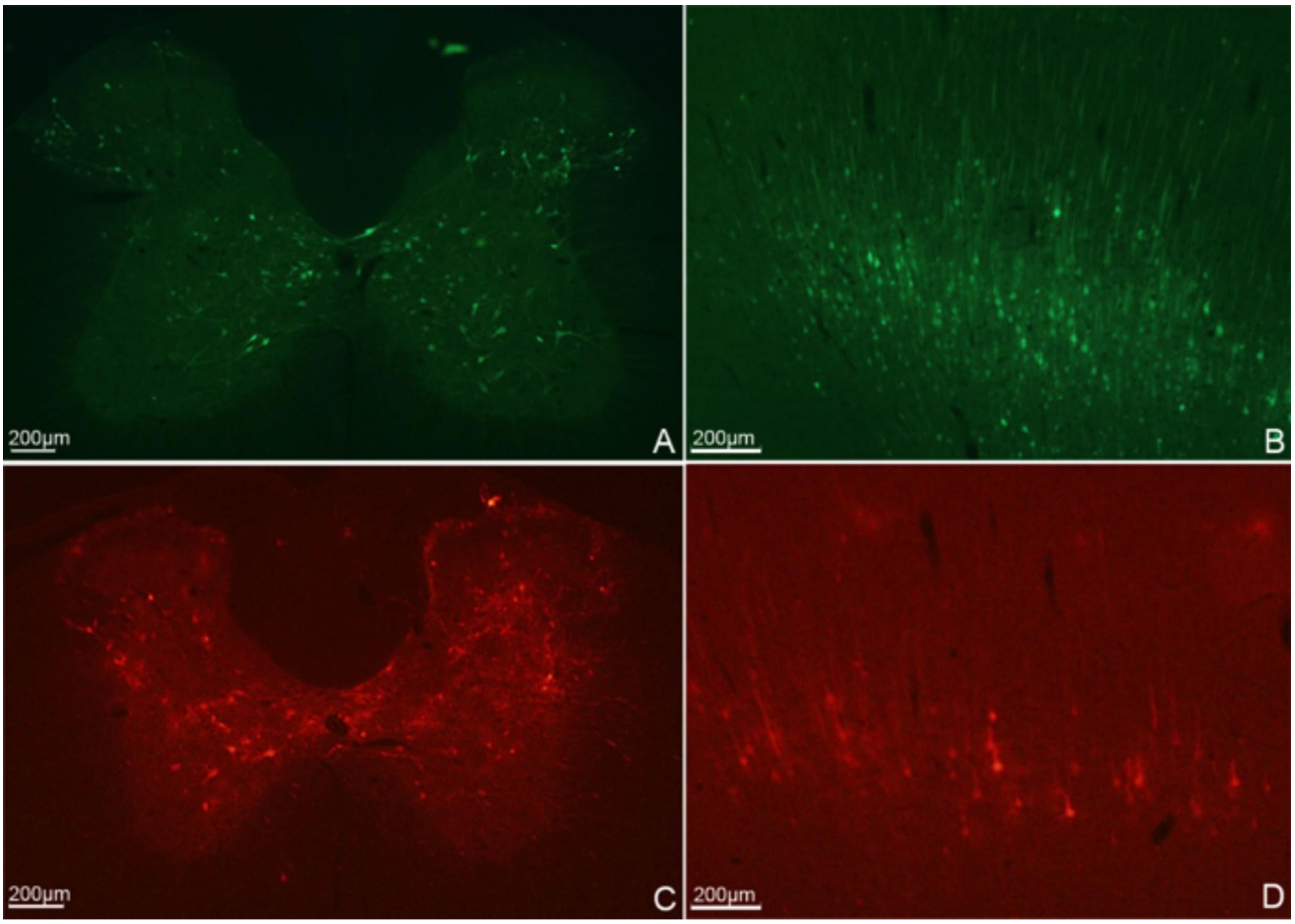


Fig. 3. Neuronal architecture in the spinal cord and M1 region of the cerebral cortex three and six days after intramuscular PRV injection: A: Spinal cord neurons three days post-PRV injection into the biceps. B: M1 region of the cerebral cortex six days post-PRV-CAG-EGFP injection into the biceps. C: Spinal cord neurons three days post-PRV-CAG-mRFP injection into the triceps. D: M1 region of the cerebral cortex six days post-PRV injection into the triceps.

**Co-injection of both muscles.** When PRV-CAG-EGFP and PRV-CAG-mRFP were co-injected into the biceps and triceps for 3 days, PRV-infected neurons in the C5-T1 segments remained primarily ipsilateral to the injection points. Neurons innervating the biceps were green (Fig. 4A), and those innervating the triceps were red (Fig. 4B). Compared to single muscle injections, the number of labeled neurons was relatively lower, but there were notable interneurons labeled with both green and red fluorescence, appearing yellow in merged images (Fig. 4C). Six days post-injection, both green- and red-labeled pyramidal cells (Figs. 4D and 4E), as well as double-color-labeled neurons, were observed in the M1 region of the cerebral cortex (Figs. 4D, 4E and 4F). The number of double-color-labelled neurons was higher than that observed in the spinal cord.

**Additional Observations.** Six days after PRV injection, numerous PRV-infected star-shaped and polygonal neurons were observed in the bilateral red nuclei, with many double-labeled neurons present among the densely distributed neurons in the red nucleus (Figs. 5A-C). Green-, red-, and double-color-labeled neurons communicated with each other through dendrites and collaterals, forming a complex neural network.

## DISCUSSION

The traditional view that the agonist muscle relaxes when the agonist muscle contracts, known as neural reciprocal inhibition, has been overly simplistic. Co-activation offers a more accurate explanation for muscle dynamics: when the flexor muscle contracts, the antagonist muscle does not merely relax but may also contract. The idea that cortical motor neurons are the sole regulators of skeletal muscle movement is now contested. Evidence suggests that brainstem and spinal cord neurons also play roles in indirect regulation. Specifically, brainstem nuclei, such as the lateral reticular and red nuclei are implicated in the co-activation pathway of skeletal muscles (Morris *et al.*, 2011; Alstermark & Pettersson, 2014).

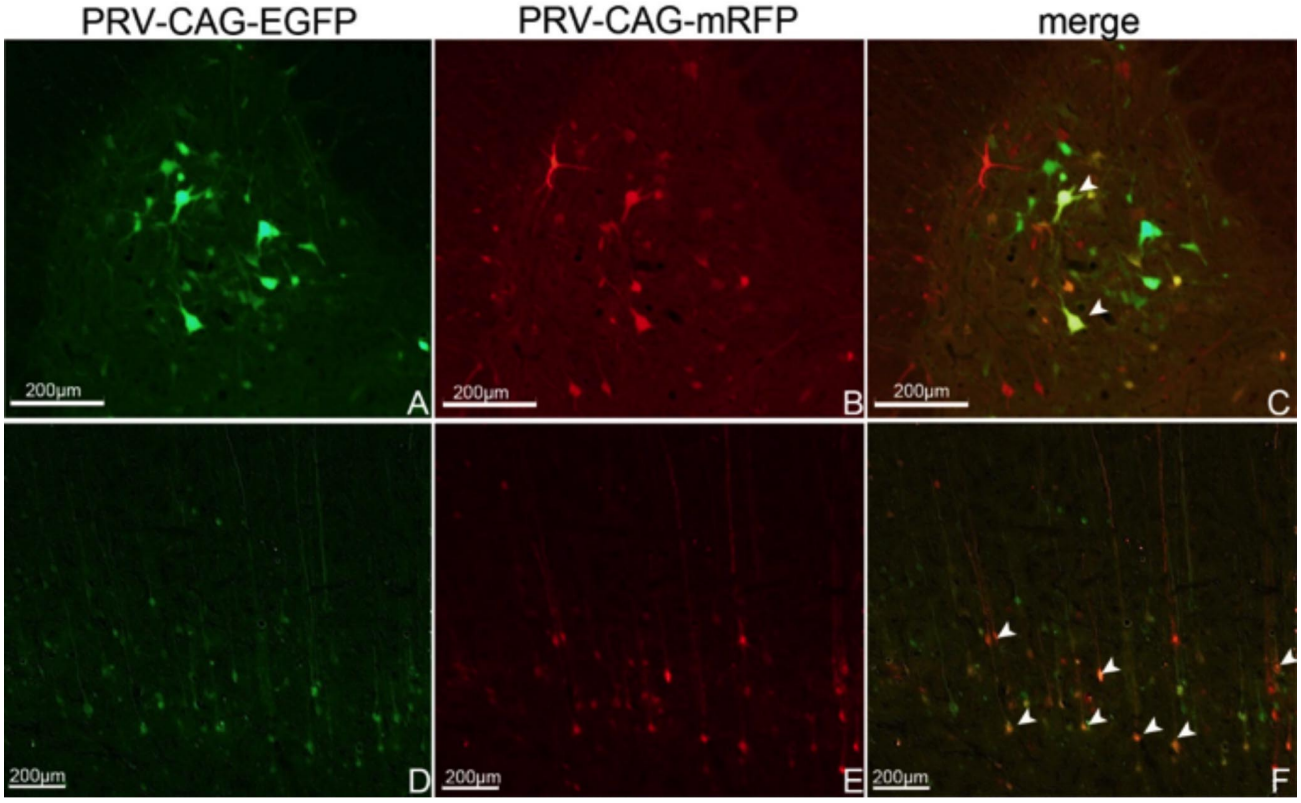


Fig. 4. Neuronal architecture in the spinal cord and M1 region of the cerebral cortex three and six days after PRV co-injection into the biceps and triceps: A: Spinal cord three days post-PRV injection into the biceps. B: Spinal cord neurons three days post-PRV injection into the triceps. C: Merged image of A and B, with arrows indicating interneurons. D: M1 region of the cerebral cortex six days post-PRV injection into the biceps. E: M1 region of the cerebral cortex six days post-PRV injection into the triceps. F: Merged image of D and E, with arrows indicating double-color-labeled neurons.

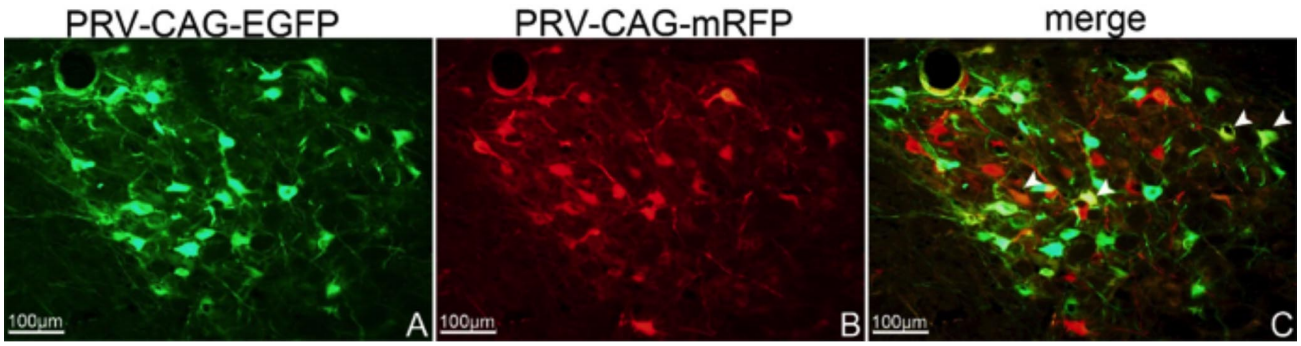


Fig. 5. Neuronal architecture in the red nucleus six days after simultaneous PRV injection into the INDRs of the biceps and triceps. A-C: Neuronal architecture after PRV-CAG-EGFP tracing, PRV-CAG-mRFP tracing, and merged images of A and B. Arrows indicate double-labeled neurons.

We hypothesized that common interneurons or collaterals between somatic motor neurons in the cerebral cortex, brainstem, and spinal cord control antagonistic muscle groups. This hypothesis posits that simultaneous excitation of neurons controlling opposing movements (e.g., flexion, extension, abduction, and contraction) results in co-activation of antagonistic muscle groups. To test this, we used the elbow flexor and extensor muscles, injecting PRV into the INDRs to retrogradely trace across multiple synapses. Observing the structural relationships between nerve cells controlling these muscles in the spinal cord, brain stem, and cerebral cortex will provide morphological evidence for the co-activation mechanism during elbow flexion.

The neuronal architectures of the spinal cord and cerebral cortices have been previously described (De Leonardis, 1951; Olivares-Moreno *et al*., 2017). Motor neurons innervating skeletal muscles are well mapped. After the location of the motor endplates was indicated by acetylcholinesterase staining, the segmental arrangement of neurons innervating the forelimb muscles of rats in the spinal cord were retrograde-traced by injecting fluorescence gold into the motor endplates. The motor neurons innervating the biceps and triceps were found to be mainly located at C3-C8 segments, especially at the C3-C5 segments, with the neuronal architecture of both muscles overlapping at the C5 level (Tosolini & Morris, 2012).

Intracortical-electrical stimulation experiments have demonstrated that the caudal region of rat M1 is associated with forelimb movement (Saiki *et al*., 2014; Kimura *et al*., 2017). Electromyographic activity of the forelimb muscles was measured after microstimulation in the cortex of rhesus monkeys. It was found that cells controlling forelimb flexor movement were mainly located in the lateral M1 region of the forelimb innervation area, while extensors were primarily in the medial area (Hudson *et al*., 2017). Other studies have shown that cortical motor neurons innervating different finger muscles in macaque monkeys overlap extensively, suggesting that this overlap and the ensuing confusion among different cortical motor neuron groups may form the neural basis for the synergistic effect between different muscles (Rathelot & Strick, 2006). Based on the consistent location of the INDRs and motor endplates (Tosolini & Morris, 2012), this study injected the PRV virus into the INDRs to trace them retrogradely across multiple synapses. The study found that the location and overlapping distribution of motor neurons innervating the biceps and triceps in the spinal cord and cortex were consistent with previous descriptions. In this experiment, neurons labeled green innervated the biceps brachii, neurons labeled red innervated the triceps brachii, and double-labeled neurons were interneurons that regulated the co-activation of both muscles.

In this study, a tracer was injected into the center of the INDRs to improve tracer absorption efficiency. However, results showed that the number of red-labeled cells in the spinal cord and cerebral cortex was slightly lower than that of green-labeled cells. This discrepancy may be due to the following reasons: (1) Only the long head of the triceps brachii was injected for ease of injection, leading to fewer nerves traced by the PRV. The nerve branches of the biceps brachii are mainly densely distributed in the long head, increasing the probability of being traced compared to the triceps brachii. (2) The PRV is a synaptic-specific trans neuronal retrograde tracer, meaning the probability of cortical motor cell tracing depends on the levels in the neural circuit and the number of nerve cells in the spinal cord being traced. PRV requires retrograde transport across the spinal cord to reach the brain when injected into both the biceps and triceps brachii muscles, resulting in prolonged viral replication and transport at the cortical level.

Skeletal muscle movement is regulated by direct and indirect neural pathways (Isa *et al*., 2007). The "direct pathway" refers to the direct connection between cerebral cortex cells and spinal motor neurons, bypassing the intermediate spinal cord neurons to induce skeletal muscle contraction (Liang *et al*., 1991; Biane *et al*., 2015). Indirect pathways include cerebral cortical motor neurons that activate interneurons in the spinal cord (Takei & Seki, 2010; Olivares-Moreno *et al*., 2017), reticulospinal tract (Alstermark *et al*., 2004), and rubrospinal tract (Whishaw *et al*., 1990). Studies have found that the motor cortex of the flexor muscle sends axon collaterals to form synaptic coupling with the motor cortex of the extensor muscle, synergistically controlling the contraction of the agonist and antagonist muscles (Capaday *et al*., 1998). In this study, double-labeled neurons in the M1 region of the cerebral cortex formed the basis of the neuronal architecture for the regulation of co-activation between the extensor and flexor muscles at the brain level. In addition, single- and double-labeled neurons were observed in the bilateral red nuclei. This phenomenon may be due to: (1) The trans polysynaptic tracer, and the rubrospinal tract's fiber that traversed from the origin of the red nucleus to the contralateral descending tract, resulted in simultaneous labeling of both sides. (2) The rubrospinal tract functions as an excitatory pathway for flexor muscles and an inhibitory pathway for extensor muscles. Single-color labeled neurons specifically regulate the biceps (flexor) and triceps (extensor) muscles, whereas double-color labeled neurons provide the neuronal architecture for the regulation of co-activation and contraction of these muscles.

This study aimed to identify the optimal injection site for multiple synaptic retrograde tracers (PRV) using a central injection of INDRs for the first time, thereby enhancing tracer efficacy. The findings demonstrate the structural relationship between nerve cells that innervate the biceps brachii (flexing elbow) and the triceps brachii (extending elbow) in the spinal cord, cerebral cortex, and red nucleus of the brainstem. The neuronal structural basis of their co-activation should be double-labeled neurons. However, whether they are interneurons and whether they provide direct evidence of co-activation needs to be further confirmed by subsequent studies. This study has several limitations. Firstly, only the long head of the triceps brachii was injected, which may not fully represent the innervation pattern of the entire muscle. Secondly, the synaptic-specific nature of PRV as a retrograde tracer and the prolonged transport time could affect the accuracy of tracing cortical motor cells.

**ACKNOWLEDGMENTS.** The authors sincerely thank for the laboratory platform provided by Zhi Xiao from the Department of Anesthesiology Zunyi Medical University.

**LI, Y.; LI, Y.; SHEN, R.; YANG, L.; HUANG, S.; XIAO, N.; YUAN, F. & YANG, S.** Arquitectura neuronal de la coactivación de los músculos flexores y extensores durante la flexión del codo revelada por el trazado PRV. *Int. J. Morphol., 42(6)*:1517-1523, 2024.

**RESUMEN:** Los mecanismos reguladores subyacentes a la cocontracción de los músculos bíceps y tríceps braquial durante la flexión del codo siguen sin estar claros. Este estudio tuvo como objetivo dilucidar las conexiones estructurales entre las células nerviosas responsables de esta coactivación. Empleamos la técnica de tinción de Sihler modificada para visualizar las regiones con alta densidad nerviosa dentro de los músculos bíceps y tríceps braquial. Además, se inyectó en estas regiones un trazador retrógrado (virus de la pseudorrabia) que expresa proteínas fluorescentes verdes y rojas mejoradas para mapear las relaciones estructurales de las células nerviosas en la médula espinal, el núcleo rojo del mesencéfalo y la región M1 de la corteza cerebral. Las regiones con mayor densidad nerviosa en los músculos bíceps y tríceps braquial se ubicaron en el 74,75 % y el 61,90 % de la longitud muscular, respectivamente. Tres días después de la inyección, observamos neuronas motoras de marca única que inervaban el bíceps (verde) y el tríceps (rojo), así como interneuronas de marca doble en el asta anterior de la médula espinal. Seis días después de la inyección, se identificaron neuronas de marca única y doble en el núcleo rojo y la corteza M1. La presencia de neuronas de marca doble tanto en la médula espinal como en las regiones cerebrales proporciona evidencia de la base neural de la coactivación en los músculos flexores y extensores durante la flexión del codo. Este estudio mejora nuestra comprensión de los mecanismos neuronales que controlan la cocontracción muscular.

**PALABRAS CLAVE: Músculo bíceps braquial; Músculo tríceps braquial; Coactivación; interneurona; Arquitectura celular neuronal.**

## REFERENCES

Alstermark, B. & Pettersson, L. G. Skilled reaching and grasping in the rat: lacking effect of corticospinal lesion. *Front Neurol., 5*:103, 2014.

Alstermark, B.; Ogawa, J. & Isa, T. Lack of monosynaptic corticomotoneuronal EPSPs in rats: disynaptic EPSPs mediated via reticulospinal neurons and polysynaptic EPSPs via segmental interneurons. *J. Neurophysiol., 91(4)*:1832-9, 2004.

Biane, J. S.; Scanziani, M.; Tuszynski, M. H. & Conner, J. M. Motor Cortex Maturation Is Associated with Reductions in Recurrent Connectivity among Functional Subpopulations and Increases in Intrinsic Excitability. *J. Neurosci., 35(11)*:4719-28, 2015.

Canedo, A. Primary motor cortex influences on the descending and ascending systems. *Prog. Neurobiol., 51(3)*:287-335, 1997.

Capaday, C.; Devanne, H.; Bertrand, L. & Lavoie, B. A. Intracortical connections between motor cortical zones controlling antagonistic muscles in the cat: a combined anatomical and physiological study. *Exp. Brain Res., 120(2)*:223-32, 1998.

Chiou, S. Y.; Wang, R. Y.; Liao, K. K.; Wu, Y. T.; Lu, C. F. & Yang, Y. R. Co-activation of primary motor cortex ipsilateral to muscles contracting in a unilateral motor task. *Clin. Neurophysiol., 124(7)*:1353-63, 2013.

De Leonardis, L. Cellular architecture of the anterior horn of the human spinal cord. *Boll. Soc. Ital. Biol. Sper., 27(5)*:752-4, 1951.

Griffin, D. M.; Hoffman, D. S. & Strick, P. L. Corticomotoneuronal cells are "functionally tuned". *Science, 350(6261)*:667-70, 2015.

Hirabayashi, R.; Kojima, S.; Edama, M. & Onishi, H. Activation of the supplementary motor areas enhances spinal reciprocal inhibition in healthy individuals. *Brain Sci., 10(9)*:587, 2020.

Hudson, H. M.; Park, M. C.; Belhaj-Saïf, A. & Cheney, P. D. Representation of individual forelimb muscles in primary motor cortex. *J. Neurophysiol., 118(1)*:47-63, 2017.

Isa, T.; Ohki, Y.; Alstermark, B.; Pettersson, L. G. & Sasaki, S. Direct and indirect cortico-motoneuronal pathways and control of hand/arm movements. *Physiology (Bethesda), 22*:145-52, 2007.

Kagamihara, Y. & Tanaka, R. Reciprocal inhibition upon initiation of voluntary movement. *Neurosci. Lett., 55(1)*:23-7, 1985.

Kimura, R.; Saiki, A.; Fujiwara-Tsukamoto, Y.; Sakai, Y. & Isomura, Y. Large-scale analysis reveals populational contributions of cortical spike rate and synchrony to behavioural functions. *J. Physiol., 595(1)*:385-413, 2017.

Lanuza, G. M.; Gosgnach, S.; Pierani, A.; Jessell, T. M. & Goulding, M. Genetic identification of spinal interneurons that coordinate left-right locomotor activity necessary for walking movements. *Neuron, 42(3)*:375-86, 2004.

Lewis, G. N.; MacKinnon, C. D.; Trumbower, R. & Perreault, E. J. Co-contraction modifies the stretch reflex elicited in muscles shortened by a joint perturbation. *Exp. Brain Res, 207(1-2)*:39-48, 2010.

Liang, F. Y.; Moret, V.; Wiesendanger, M. & Rouiller, E. M. Corticomotoneuronal connections in the rat: evidence from double-labeling of motoneurons and corticospinal axon arborizations. *J. Comp. Neurol., 311(3)*:356-66, 1991.

Morris, R.; Tosolini, A. P.; Goldstein, J. D. & Whishaw, I. Q. Impaired arpeggio movement in skilled reaching by rubrospinal tract lesions in the rat: a behavioral/anatomical fractionation. *J. Neurotrauma, 28(12)*:2439-51, 2011.

Olivares-Moreno, R.; Moreno-Lopez, Y.; Concha, L.; Martínez-Lorenzana, G.; Condés-Lara, M.; Cordero-Erausquin, M. & Rojas-Piloni, G. The rat corticospinal system is functionally and anatomically segregated. *Brain Struct. Funct., 222(9)*:3945-58, 2017.

Pincivero, D. M.; Polen, R. R. & Byrd, B. N. Contraction mode and intensity effects on elbow antagonist muscle co-activation. *J. Electromyogr. Kinesiol., 44*:101-7, 2019.

Rathelot, J. A. & Strick, P. L. Muscle representation in the macaque motor cortex: an anatomical perspective. *Proc. Natl. Acad. Sci. U. S. A., 103(21)*:8257-62, 2006.

Saiki, A.; Kimura, R.; Samura, T.; Fujiwara-Tsukamoto, Y.; Sakai, Y. & Isomura, Y. Different modulation of common motor information in rat primary and secondary motor cortices. *PLoS One, 9(6)*:e98662, 2014.

Takei, T. & Seki, K. Spinal interneurons facilitate coactivation of hand muscles during a precision grip task in monkeys. *J. Neurosci., 30(50)*:17041-50, 2010.

Tosolini, A. P. & Morris, R. Spatial characterization of the motor neuron columns supplying the rat forelimb. *Neuroscience, 200*:19-30, 2012.

Whishaw, I. Q.; Tomie, J. A. & Ladowsky, R. L. Red nucleus lesions do not affect limb preference or use, but exacerbate the effects of motor cortex lesions on grasping in the rat. *Behav. Brain Res., 40(2)*:131-44, 1990.

Yu, J.; Li, Y.; Yang, L.; Li, Y.; Zhang, S. & Yang, S. The highest region of mucle spindle abundance should be the optimal target of botulinum toxon A injection to block muscle spasms in rats. *Front. Neurol., 14*:1061849, 2023

Corresponding author:
Shengbo Yang
Department of Anatomy Zunyi Medical University
6 West Xufu Road
Xinpu Developing Zones
Zunyi 563099
CHINA

E-mail: yangshengbo8205486@163.com